

Classification and Complete Solution of the Kinetostatics of a Compliant Stewart-Gough Platform

Hafez Tari^{a,1}, Hai-Jun Su^{b,2}, Jonathan D. Hauenstein^{c,3}

^a*Department of Mechanical Engineering,
The Ohio State University,
Columbus, OH 43210, USA*

^b*Department of Mechanical Engineering,
University of Maryland, Baltimore County,
Baltimore, MD 21250, USA*

^c*Department of Mathematics,
Texas A&M University,
College Station, TX 77843, USA*

Dedicated to Prof. Joseph Duffy.

Abstract

This paper studies a compliant Stewart-Gough platform whose six flexible links balance external loads, including force and moment, applied to a general point at the platform. Soma coordinates are used to express the location of the moving plate with respect to the base plate. The mathematical modeling involves both the kinematics and the statics. Seven kinematic and six static constraints are obtained. Vector dot- and cross-products are also cast in quaternion form which reduce the degree of the resulting constraints. By classifying the parameters to the knowns and the unknowns, five major problem types are recognized. Four of them are mathematically decoupled and the remaining one is coupled for which the obtained 13 polynomials are of the total degree of 5,971,968 which to the authors' best of knowledge is the largest kinematic problem ever investigated. After solving the equations with the numerical polynomial solver Bertini, we conclude that the upper bound to the number of nonsingular solutions is 29,272. In addition, for practical problems a parameter continuation is devised to recompute for only 29,272 generically nonsingular solutions. At last a numerical example is provided to demonstrate the solution process.

Key words: Compliant Stewart-Gough Platform, Kinematics, Kinetostatics, Stiffness Mapping, Soma Coordinates, Numerical Continuation.

¹Email: tari.1@osu.edu, Tel.: +1 614 292 2289, Address all correspondence to this author

²Email: haijun@umbc.edu

³Email: jhauenst@math.tamu.edu

Nomenclature

i An integer index taking value 0 through 5

j An integer index taking value 1 through 5

1. Introduction

Stewart-Gough platforms [1, 2] are formed by connecting a moving platform link or stage to a fixed ground link via six limbs that are actuated with prismatic joints. They are frequently used in applications such as the flight simulations. On the other hand, compliant platform mechanisms are parallel linked mechanisms [3] with one or more flexible limbs or joints which are designed to deform under an external loading. They can be found in various applications including tensegrity systems [4, 5, 6], remote center compliance devices [7] for industrial robots, statically balanced devices [8] and so on.

Numerous pieces of work have been done on the kinematics of traditional or rigid body Stewart-Gough platforms. The two main kinematic problems are called inverse (indirect) kinematics and forward (direct) kinematics. It is well known that the former is relatively easy while the latter is rather challenging. One of the earliest solution to the forward kinematics of the most general case was conducted by Raghavan [9] who found 40 generic configurations using the numerical continuation method [10, 11, 12, 13]. The same result was found later with employing Gröbner basis method [14, 15]. Wampler [16] also formulated the problem with soma coordinates [17] and verified the same result by deriving the 2-homogeneous Bezout number. These results stimulated the derivation of other resultant elimination solutions by Husty [18], Innocenti [19] and others [20, 21]. Very recently, Tari and Su [22] constructed a solution library for solving the forward kinematics of the entire Stewart-Gough platform topologies with a recently developed homotopy solver Bertini [23].

However, there are relatively less pieces of work on the analysis and design of compliant platforms. Unlike the classical platforms, the analysis of compliant platforms requires both kinematic analysis and static equilibrium analysis, which we call the “kinetostatic analysis”. The former is essentially the same as that of the rigid body platform. While the latter studies the relation between the external loading and the mechanism configuration defined by its generalized coordinates. Moreover, the concept of the stiffness/compliance mapping comes into play once the static deformation due to an external loading is sufficiently small. This is what we call the “instantaneous or local static analysis”. In this area, Patterson and Lipkin [24] systematically studied compliance matrices of robots. Huang and Schimmels [25] studied the synthesis of a compliance matrix with simple springs connected in serial or in parallel.

However, here we are interested in the “finite or global static analysis” problem in which both the position and the orientation of the platform link and the deformation of compliant limbs are unknown. In this area, Pigoski and Duffy [26] formulated the planar two-spring problem consisting of point connect to ground by two compliant limbs and obtained a closed-form solution which led to as many as six equilibrium configurations for a given external load. Sun et al. [27] extended this problem and studied a planar three-spring system with a moving platform consisting of a line segment for which a maximum

of 54 equilibrium configurations is reported. The most general case of planar compliant platforms was studied in Ref. [28] and using the numerical continuation it was concluded that there can be as many as 70 equilibrium positions for a given loading applied to the platform. With regard to spatial compliant platforms, Zhang et al. [29] studied a special case with three linear springs joined at the same point on the platform.

The problem to be solved in this paper is described as what follows. Given a compliant Stewart-Gough platform with six compliant limbs modeled as six linear springs, and given a general external loading (force and moment) applied to the platform link, we would like to find all possible equilibrium configurations of the mechanism.

The rest of the paper is organized as follows. Next we give vector dot- and cross-products using quaternion algebra. Section 3 introduces the compliant Stewart-Gough platform and derives its kinetostatics. Section 4 gives the problem statements and the underlying constraints and a solution procedure for each problem type. A numerical example is given in section 5.

2. Vector Dot- and Cross-Products with Quaternion Algebra

Any four-tuple of real numbers Q_0, Q_1, Q_2 and Q_3 , as in Ref. [17] or many other available textbooks, is denoted as a quaternion $\hat{Q} = (Q_0, \mathbf{Q})$ where $Re(\hat{Q}) = Q_0$ and $Vec(\hat{Q}) = \mathbf{Q} = (Q_1, Q_2, Q_3)$ are called the real and the vector parts of \hat{Q} , respectively. Moreover, the conjugate of \hat{Q} is defined as $\hat{Q}' = (Q_0, -\mathbf{Q})$. Additionally, the quaternion \hat{Q} is called a unit quaternion if $\hat{Q}^T \hat{Q} = 1$ where “ T ” is the transpose operator. Finally, a pure vector quaternion is a quaternion whose real part is zero and we show it as $\hat{Q}_v = (0, \mathbf{Q})$.

Addition of the two quaternions $\hat{Q}^1 = (Q_0^1, \mathbf{Q}^1)$ and $\hat{Q}^2 = (Q_0^2, \mathbf{Q}^2)$ is carried out element-wise, i.e. $\hat{Q}^1 + \hat{Q}^2 = (Q_0^1 + Q_0^2, \mathbf{Q}^1 + \mathbf{Q}^2)$, and their product, which is again a quaternion, shown by the symbol “ $*$ ” is carried out in terms of vector dot- and cross-products as

$$\hat{Q}^1 * \hat{Q}^2 = (Q_0^1 Q_0^2 - \mathbf{Q}^1 \cdot \mathbf{Q}^2, Q_0^1 \mathbf{Q}^2 + Q_0^2 \mathbf{Q}^1 + \mathbf{Q}^1 \times \mathbf{Q}^2). \quad (1)$$

For any three-dimensional vector \mathbf{v} and R , a 3×3 orthogonal rotation matrix, there is a unit quaternion \hat{q} such that

$$R\mathbf{v} = \hat{q} * \mathbf{v} * \hat{q}', \quad (2)$$

where R is as follows.

$$R = \begin{bmatrix} q_0^2 + q_1^2 - q_2^2 - q_3^2 & 2(q_1 q_2 - q_0 q_3) & 2(q_0 q_2 + q_1 q_3) \\ 2(q_1 q_2 + q_0 q_3) & q_0^2 - q_1^2 + q_2^2 - q_3^2 & 2(q_2 q_3 - q_0 q_1) \\ 2(q_1 q_3 - q_0 q_2) & 2(q_0 q_1 + q_2 q_3) & q_0^2 - q_1^2 - q_2^2 + q_3^2 \end{bmatrix} \quad (3)$$

Moreover, once the rotation of R is combined with a pure displacement \mathbf{p} , we use the quaternion $\hat{g} = (g_0, \mathbf{g})$ where

$$0 = Re(\hat{g} * \hat{q}') = \hat{g}^T \hat{q} \quad (4)$$

$$\mathbf{p} = Vec(\hat{g} * \hat{q}') = q_0 \mathbf{g} - g_0 \mathbf{q} + \mathbf{q} \times \mathbf{g}. \quad (5)$$

The terms $\mathbf{p} \cdot \mathbf{p}$, $R\mathbf{v} \cdot \mathbf{p}$ and $R\mathbf{v} \times \mathbf{p}$ require further attention as they play major roles in the complexity, i.e. the degree of the nonlinearity, of the kinetostatic equations which govern the behavior of the compliant Stewart-Gough platform to be studied later. For example, both $R\mathbf{v} \cdot \mathbf{p}$ and $R\mathbf{v} \times \mathbf{p}$ seem to be fourth-degree in terms of the unknown quaternions \hat{g} and \hat{q} while in the following we show that both of them are actually quadratic.

It follows from Eq. (1) that the vector dot- and cross-products of two vectors \mathbf{Q}_1 and \mathbf{Q}_2 can also be obtained from the product of their pure vector quaternions as

$$\mathbf{Q}_1 \cdot \mathbf{Q}_2 = Re(\hat{Q}_v^1 * \hat{Q}_v^{2'}) \quad (6)$$

$$\mathbf{Q}_1 \times \mathbf{Q}_2 = -Vec(\hat{Q}_v^1 * \hat{Q}_v^{2'}). \quad (7)$$

Recall that \hat{q} is a unit quaternion, it is clear from Eqs. (5) and (6) that

$$\mathbf{p} \cdot \mathbf{p} = Re(\hat{g} * \hat{q}' * \hat{q} * \hat{g}') = Re(\hat{g} * \hat{g}') = \hat{g}^T \hat{g}. \quad (8)$$

In addition, according to Eqs. (2), (5), (6) and (7) and considering the fact that $(\hat{Q}^1 * \hat{Q}^2)' = \hat{Q}^{2'} * \hat{Q}^1'$, it is not hard to see that

$$R\mathbf{v} \cdot \mathbf{p} = Re(\hat{q} * \mathbf{v} * \hat{q}' * \hat{q} * \hat{g}') = Re(\hat{q} * \mathbf{v} * \hat{g}') = \tilde{\mathbf{g}}^T \mathbf{v} \quad (9)$$

$$R\mathbf{v} \times \mathbf{p} = -Vec(\hat{q} * \mathbf{v} * \hat{q}' * \hat{q} * \hat{g}') = -Vec(\hat{q} * \mathbf{v} * \hat{g}') = G\mathbf{v}. \quad (10)$$

where

$$\tilde{\mathbf{g}}^T = [g_1 q_0 - g_0 q_1 - g_3 q_2 + g_2 q_3 \quad g_2 q_0 + g_3 q_1 - g_0 q_2 - g_1 q_3 \quad g_3 q_0 - g_2 q_1 + g_1 q_2 - g_0 q_3] \quad (11)$$

$$G = \begin{bmatrix} 2(g_2 q_2 + g_3 q_3) & g_3 q_0 - g_2 q_1 - g_1 q_2 + g_0 q_3 & -(g_2 q_0 + g_3 q_1 + g_0 q_2 + g_1 q_3) \\ -(g_3 q_0 + g_2 q_1 + g_1 q_2 + g_0 q_3) & 2(g_1 q_1 + g_3 q_3) & g_1 q_0 + g_0 q_1 - g_3 q_2 - g_2 q_3 \\ g_2 q_0 - g_3 q_1 + g_0 q_2 - g_1 q_3 & -(g_1 q_0 + g_0 q_1 + g_3 q_2 + g_2 q_3) & 2(g_1 q_1 + g_2 q_2) \end{bmatrix} \quad (12)$$

3. A Compliant Stewart-Gough Platform and its Kinetostatics

Figure 1 shows a schematic view of a compliant Stewart-Gough manipulator with generic force and moment applied to a general point of the moving platform. As is seen, the manipulator like its traditional rigid counterpart consists of six prismatic links, with initial and final lengths of l_{0i} and l_i . Via spherical or ball-in-socket joints, the links are

connected at one end to the stationary platform at points \mathbf{a}_i and at the other end to the moving platform at points \mathbf{b}_i . The points \mathbf{a}_i and \mathbf{b}_i are local respectively to the base and the end plates' coordinate systems. However, unlike the rigid Stewart-Gough manipulator, the compliant Stewart-Gough manipulator features flexible legs of stiffness, k_i , which balance the globally defined external load, \mathbf{F} and \mathbf{M} , applied to the moving platform at \mathbf{b}_6 . Note, however, that a fully compliant Stewart-Gough platform which further possesses compliant spherical joints may also be articulated but is beyond the scope of this article.

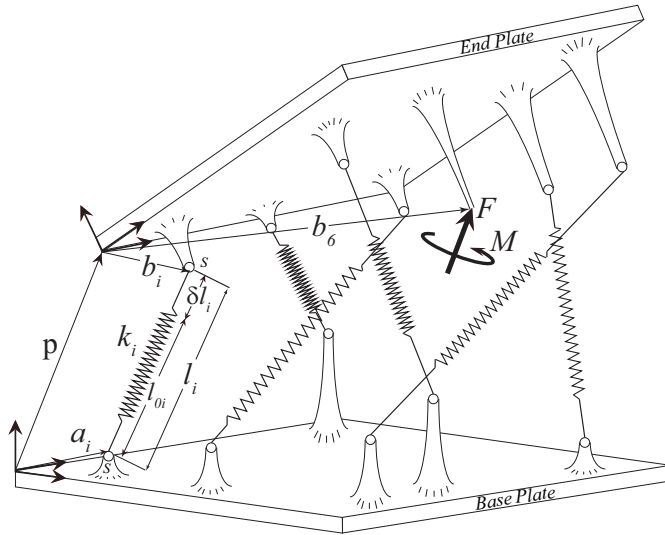


Figure 1: A schematic view of a general compliant Stewart-Gough platform

It is well known that any point \mathbf{b}_i on the moving platform may be measured in the base plate as \mathbf{B}_i using two parameters such as the vector \mathbf{p} and the quaternion \hat{q} . These parameters respectively define the position and the orientation of the moving plate with respect to the base plate as follows.

$$\mathbf{B}_i = \mathbf{p} + R\mathbf{b}_i, \quad (13)$$

where R and \mathbf{p} are as before and given by Eqs. (3) and (5), respectively.

Since the compliant Stewart-Gough platform features compliant members, its mathematical modeling involves both kinematic and static derivations as follows.

3.1. Kinematic Constraints

The kinematic constraints are common to both rigid and compliant Stewart-Gough platforms. Quite well-known, the kinematic constraints are the squared distances between the points \mathbf{a}_i and \mathbf{b}_i which equal to l_i^2 . Without loss of generality, we set $\mathbf{a}_0 = \mathbf{b}_0 = 0$. Exploiting Eqs. (4), (8), (9) and (13) and the orthogonality of R , i.e. $R^T R = R R^T = I$

where I is the 3×3 identity matrix, it is not hard to show that the following 7 quadrics constitute the kinematic constraints in the projective space \mathbb{P}^7 .

$$\begin{aligned} 0 &= \hat{g}^T \hat{q} \\ 0 &= \hat{q}^T \hat{q} l_0^2 - \hat{g}^T \hat{g} \\ 0 &= [\mathbf{B}_j - \mathbf{a}_j]^T [\mathbf{B}_j - \mathbf{a}_j] - l_j^2 \quad j=1, \dots, 5 \\ &= 2(\tilde{\mathbf{g}}^T \mathbf{b}_j - \mathbf{a}_j^T [\mathbf{p} + R\mathbf{b}_j]) + (\mathbf{a}_j^T \mathbf{a}_j + \mathbf{b}_j^T \mathbf{b}_j + l_0^2 - l_j^2) \hat{q}^T \hat{q} \end{aligned} \quad (14)$$

where the first equation follows from the orthogonality of the quaternions \hat{g} and \hat{q} . Note that the equations are homogenized considering the fact that \hat{q} is a unit quaternion which imposes the side condition $\hat{q}^T \hat{q} \neq 0$.

3.2. Static Constraints

Figure 2 illustrates the upper section of the free body diagram of the compliant Stewart-Gough manipulator. As shown, the i^{th} link at the cutting point reveals a general internal force \mathbf{f}_i with a magnitude of f_i and along the direction of the link from the point \mathbf{b}_i to \mathbf{a}_i . Summing the resultant of the forces and taking moment with respect to an arbitrary point, but for the sake of simplicity the point $\mathbf{b}_0 = 0$, and equating them to zero and also taking Eq. (10) into account result in the following equations of equilibrium.

$$F = \sum_{i=0}^5 \frac{f_i}{l_i} [\mathbf{B}_i - \mathbf{a}_i] = \frac{f_0}{l_0} \mathbf{p} + \sum_{j=1}^5 \frac{f_j}{l_j} [\mathbf{p} - \mathbf{a}_j + R\mathbf{b}_j], \quad (15)$$

$$\begin{aligned} \mathbf{M} + R\mathbf{b}_6 \times F &= \sum_{j=1}^5 \frac{f_j}{l_j} R\mathbf{b}_j \times [\mathbf{B}_j - \mathbf{a}_j] = \sum_{j=1}^5 \frac{f_j}{l_j} R\mathbf{b}_j \times [\mathbf{p} - \mathbf{a}_j] \\ &= \sum_{j=1}^5 \frac{f_j}{l_j} [G\mathbf{b}_j + \mathbf{a}_j \times R\mathbf{b}_j], \end{aligned} \quad (16)$$

where \mathbf{p} and G are respectively given by Eqs. (5) and (12) and “ \times ” denotes the vector cross-product operator. Recall that Eqs. (15) and (16) are each three-dimensional vector equation, there are in total six static constraints which require the platform to be in equilibrium under the exertion of the external load \mathbf{F} and \mathbf{M} .

The obtained static equations are clearly valid for any general internal forces of the links for this particular compliant Stewart-Gough platform. This in return enables us to consider large and finite deformations for the platform’s entire workspace. Though, the internal forces and their nonlinearity structure are application based and depend on the material and the geometry of the links involved. However, for the sake of the simplicity of the problem study given below we consider the links to be elastic meaning that $f_i = k_i \delta l_i = k_i (l_i - l_{0i})$.

4. Category of Kinetostatic Problems

The kinetostatics of a compliant Stewart-Gough platform like the kinematics of the traditional Stewart-Gough platform may be categorized depending on which parameters

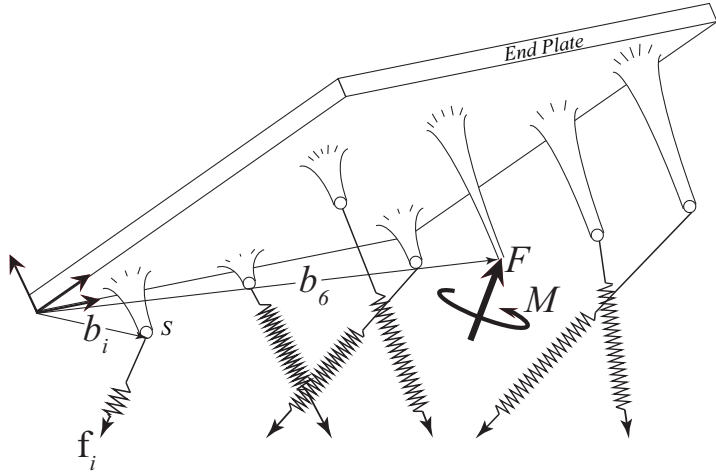


Figure 2: A schematic view of the upper section of the free body diagram of a general compliant Stewart-Gough platform

are known and which are not. Recall that for the traditional Stewart-Gough platform, the inverse kinematics is to find the legs length to achieve a desired configuration while the forward kinematics is completely opposite. In a verbatim manner, we define and add two more notions to the concepts of the forward and the inverse kinematics as follows.

Definition 1. *Pure Inverse statics* is to find the legs stiffness for prescribed external load.

Definition 2. *Pure Forward statics* is to find the external load for prescribed legs stiffness.

Exploiting the word “pure” in the foregoing definitions is crucial in that it decouples the concepts of the kinematics and the statics which as a result would drastically ease the later study. In addition, it would help avoid confusion with some common definitions in the literature which emphasize that the forward and the inverse statics study the relation between the external load and the platform configuration which obviously intertwine the kinematics and the statics. However, for succinctness from this point on, we drop the word pure from the definitions and by the forward and the inverse statics we actually mean the pure forward and the pure inverse statics, respectively.

With these concepts in mind, we categorize the kinetostatics of the compliant Stewart-Gough platforms to five major types. Surprisingly enough, the first four types lead to mathematically decoupled kinematic and static equations. We elaborate each type as follows.

4.1. Inverse-Inverse Kinetostatics: Inverse Kinematics and Inverse Statics

The goal of the inverse-inverse kinetostatics which is the combination of the inverse kinematics and the inverse statics is to find the legs length and stiffness which balance given external loads at the desired position and orientation of the moving platform w.r.t. the stationary plate. In this respect, we define $\psi^{IIK} = \{l_{0i}, \mathbf{a}_i, \mathbf{b}_i, \hat{\mathbf{b}}_6, \hat{q}, \hat{g}, \mathbf{F}, \mathbf{M}\}$ which

includes 59 known parameters and the goal is to find the entire unknown sets $\varphi^{IHK} = \{l_i, k_i\}$ which define statically balanced configurations.

The solution procedure in this case is very easy as the kinematic and the static constraint equations are decoupled. At first, one would independently solve the last six polynomials of Eq. (14) which leads to a single set of lengths l_i . Insertion of the obtained lengths to Eqs. (15) and (16) results in a linear system and upon solution would give a single set of stiffnesses k_i .

4.2. Inverse–Forward Kinetostatics: Inverse Kinematics and Forward Statics

The goal of the inverse–forward kinetostatics which is the combination of the inverse kinematics and the forward statics is to find the legs length and the external loads which lead to the desired balanced platform configurations of known stiffness and location. Therefore, the new parameter set $\psi^{IFK} = \{l_{0i}, \mathbf{a}_i, \mathbf{b}_i, \mathbf{b}_6, \hat{q}, \hat{g}, k_i\}$ still includes 59 known parameters and the goal is to find the entire unknown sets $\varphi^{IFK} = \{l_i, \mathbf{F}, \mathbf{M}\}$.

The solution procedure in this case is mathematically even simpler than that of the inverse–inverse kinetostatics as the force and the moment constraints are further decoupled. Once the legs length l_i are obtained from Eq. (14), one may proceed with obtaining the unknown vector \mathbf{F} directly from the linear system Eq. (15) and then solve Eq. (16) which is again a linear system for the external moment \mathbf{M} .

4.3. Forward–Inverse Kinetostatics: Forward Kinematics and Inverse Statics

The forward–inverse kinetostatics combines the forward kinematics and the inverse statics and its goal is to find the legs stiffness and the statically balanced location of the moving platform for given external loads and legs length. In this respect, the parameter set $\psi^{FIK} = \{l_{0i}, l_i, \mathbf{a}_i, \mathbf{b}_i, \mathbf{b}_6, \mathbf{F}, \mathbf{M}\}$ includes 57 known parameters and the goal is to find the entire unknown sets $\varphi^{FIK} = \{\hat{q}, \hat{g}, k_i\}$.

While the solution procedure in this case is similar to that of the inverse–inverse kinetostatics, the kinematic equations (Eq. 14) should be solved for the unknowns \hat{q}, \hat{g} which are well-known to have 40 nonsingular solutions. These solutions in return due to the linearity of Eqs. (15) and (16) would give rise to 40 solutions for the legs stiffness k_i .

4.4. Forward–Forward Kinetostatics: Forward Kinematics and Forward Statics

The forward–forward kinetostatics intertwines the forward kinematics and the forward statics and its goal is to find the required external loads and the resulting statically balanced location of the moving platform for the given legs length and stiffness. The parameter set $\psi^{FFK} = \{l_{0i}, l_i, \mathbf{a}_i, \mathbf{b}_i, \mathbf{b}_6, k_i\}$ includes 57 known parameters and the goal is to find the entire unknown sets $\varphi^{FFK} = \{\hat{q}, \hat{g}, \mathbf{F}, \mathbf{M}\}$.

Similar to the inverse–forward Kinetostatics, the loading equations are even decoupled hence resulting in a mathematically simpler and more efficient solution procedure. The 40 unknown vectors \mathbf{F} would be obtained upon the insertion of the already obtained 40 solutions \hat{q}, \hat{g} of Eq. (14) into the linear system of Eq. (15). Then the 40 sets of the external moments \mathbf{M} would be derived from the linear system of Eq. (16).

4.5. Coupled Kinetostatics

All of the cases considered so far led to mathematically decoupled formulations. However, it would no longer be a decoupled case if one assigned the parameter set as $\psi = \{l_{0i}, \mathbf{a}_i, \mathbf{b}_i, \mathbf{b}_6, \mathbf{F}, \mathbf{M}, k_i\}$ which contains 57 known parameters. The goal of this case which we simply call a coupled kinetostatics is to find $\varphi = \{\hat{q}, \hat{g}, l_i\}$ which would result in statically balanced configurations.

To obtain the entire solution set to this case a simultaneous solution procedure is inevitable. Therefore, with letting $\tilde{l}_i = \frac{l_{0i}}{l_i}$ we convert the constraints to the required polynomial form and rewrite the kinematic and the static constraints given in Eqs. (14), (15) and (16) as follows.

$$\mathcal{F}(\tilde{\varphi}) : \left\{ \begin{array}{lcl} \hat{g}^T \hat{q} & = & 0 \\ \hat{q}^T \hat{q} l_{00}^2 - \hat{g}^T \hat{g} \tilde{l}_0^2 & = & 0 \\ \mathbf{F} - k_0(1 - \tilde{l}_0)\mathbf{p} - \sum_{j=1}^5 k_j(1 - \tilde{l}_j)[\mathbf{p} - \mathbf{a}_j + R\mathbf{b}_j] & = & 0 \\ \mathbf{M} - \mathbf{F} \times R\mathbf{b}_6 - \sum_{j=1}^5 k_j(1 - \tilde{l}_j)[G\mathbf{b}_j + \mathbf{a}_j \times R\mathbf{b}_j] & = & 0 \\ l_{0j}^2 - (\hat{g}^T \hat{g} - \mathbf{a}_j^T [2\mathbf{p} - \mathbf{a}_j + 2R\mathbf{b}_j] + \mathbf{b}_j^T [\mathbf{b}_j + 2\tilde{\mathbf{g}}])\tilde{l}_j^2 & = & 0, \quad j = 1, \dots, 5 \end{array} \right. \quad (17)$$

With $\tilde{\varphi} = \{\hat{q}, \hat{g}, \tilde{l}_i\}$ as the variable set, the polynomial system $\mathcal{F}(\tilde{\varphi})$ is a system of 13 polynomials in $\mathbb{C}^6\mathbb{P}^7$ where \mathbb{C} and \mathbb{P} are the complex and projective spaces, respectively. Note that the total degree of $\mathcal{F}(\tilde{\varphi})$ is $2 \times 4 \times 3^3 \times 3^3 \times 4^5 = 5,971,968$ whose solution appears to be challenging even with the current state-of-the-art computers.

To solve $\mathcal{F}(\tilde{\varphi})$ we firstly defined a generic input parameter set ψ_1 , in our case with 400 numerical digits, and employed Bertini [23, 30] with its built-in regeneration mode [31]. However, to avoid round-off errors in computation of the intermediate Jacobian matrices, we implemented the polynomials in the straight-line form [32] and adopted very tight tolerances for the path tracker settings as follows. We employed the adaptive precision of Bertini and set the tracking tolerances before and during endgame to 10^{-8} and 10^{-9} , the admissible residual function evaluation tolerance to 10^{-13} and the maximum number of function evaluations to 20000. Moreover, the solution endpoints were sharpened during the path-tracking to be correct up to 30 digits. Finally, as far as the computer platform, we used the parallel version of Bertini on “tara” the newly purchased cluster of the High Performance Computing facility of the University of Maryland, Baltimore County.

As a result, after tracing and moving respectively 253,602 and 190,162 solution paths, Bertini finally returned 29,272 nonsingular and finite solutions, i.e. only 6.6% of the total paths. On the other hand, the numerical continuation methods, which Bertini actually employs, are probability-one methods [10, 11, 12, 13] meaning that they may fail only for certain numerical values of the involved parameters. Hence, after repeating this step for several new input parameters and obtaining the same number of solutions, we conclude that the upper bound to the number of solutions to the coupled kinetostatics of a general compliant Stewart-Gough platform is 29,272.

It would be impractical if the solution of $\mathcal{F}(\tilde{\varphi})$ for a newly defined parameter set ψ_2 required repeating for the computation of the extra 93.4% junk paths. Since ψ_1 is general, the theory of parameter homotopies (see [13]) states that the nonsingular solutions of $\mathcal{F}(\tilde{\varphi}, \psi_2)$ can be obtained by following the solution paths of $\mathcal{F}(\tilde{\varphi}, (1-s)\psi_1 + s\psi_2)$ starting

at the 29,272 nonsingular solutions of $\mathcal{F}(\tilde{\varphi}, \psi_1)$ as the real parameter s increments from 0 to 1.

4.5.1. Discussion

1. While the maximum number of assembly configurations of a general rigid Stewart-Gough platform is 40, there are special geometries which attain only eight assembly configurations [22]. But regardless of the compliance, rigid and compliant Stewart-Gough platforms share a common topology and it makes sense compliant Stewart-Gough platforms of less general geometries possess less assembly configurations than 29,272.
2. Once solving $\mathcal{F}(\tilde{\varphi})$ numerically, the computations were carried out in the complex and the projective domains which would explain the fact that not the entire 29,272 configurations be physically attainable in the real domain. Even if the entire 29,272 solutions are real, not all of them may be valid since they should result in positive displaced leg length components l_i .
3. It is clear that if $\{\hat{q}, \hat{g}, \tilde{l}_i\}$ is a solution set to $\mathcal{F}(\tilde{\varphi})$ so will be $\{-\hat{q}, -\hat{g}, \tilde{l}_i\}$ as it leaves $\mathcal{F}(\tilde{\varphi})$ unchanged. This is in agreement with the forward kinematics of the rigid Stewart-Gough platforms as well. Therefore, with twice endeavor one would have obtained twice as many solutions as 29,272 if the formulation was done in the complex space \mathbb{C}^{14} .
4. Considering the complexity of deriving a 40th degree univariate polynomial for the forward kinematics of rigid Stewart-Gough platforms, obtaining closed form solutions or a univariate polynomial of 29,272th degree for the coupled kinetostatics of compliant Stewart-Gough platforms seems infeasible. This may justify the use of the numerical continuation as the only means of the solution tool for the coupled kinetostatics of compliant Stewart-Gough platforms.
5. Further reduction of $\mathcal{F}(\tilde{\varphi})$ is possible with some elimination steps. For example, one may linearly solve the static equations to eliminate the variables \tilde{l}_i . This reduces \mathcal{F} to 7 equations but this is not numerically advantageous.

A summary of all five kinetostatic problems is tabulated in Table 1. Note that, for conciseness, we have grouped parameters as $\mathbf{l}_0 = \{l_{00}, \dots, l_{05}\}$, $\mathbf{l} = \{l_0, \dots, l_5\}$, $\mathbf{k} = \{k_0, \dots, k_5\}$ and $\tilde{\mathbf{l}} = \{\frac{l_{00}}{l_0}, \dots, \frac{l_{05}}{l_5}\}$.

Table 1: Five kinetostatic problems of the compliant Stewart-Gough platform

Kinetostatics problem type	Known parameters	Unknowns	Solution procedure: Solve Eqs.	# of sols.
Inv.-Inv.	$\{\mathbf{l}_0, \mathbf{a}, \mathbf{b}, \hat{q}, \hat{g}, \mathbf{F}, \mathbf{M}\}$	$\{\mathbf{l}, \mathbf{k}\}$	(i) 14 (ii) 15,16	1
Inv.-Fwd.	$\{\mathbf{l}_0, \mathbf{a}, \mathbf{b}, \hat{q}, \hat{g}, \mathbf{k}\}$	$\{\mathbf{l}, \mathbf{F}, \mathbf{M}\}$	(i) 14 (ii) 15 (iii) 16	1
Fwd.-Inv.	$\{\mathbf{l}_0, \mathbf{l}, \mathbf{a}, \mathbf{b}, \mathbf{F}, \mathbf{M}\}$	$\{\hat{q}, \hat{g}, \mathbf{k}\}$	(i) 14 (ii) 15,16	40
Fwd.-Fwd.	$\{\mathbf{l}_0, \mathbf{l}, \mathbf{a}, \mathbf{b}, \mathbf{k}\}$	$\{\hat{q}, \hat{g}, \mathbf{F}, \mathbf{M}\}$	(i) 14 (ii) 15 (iii) 16	40
Coupled	$\{\mathbf{l}_0, \mathbf{a}, \mathbf{b}, \mathbf{F}, \mathbf{M}, \mathbf{k}\}$	$\{\tilde{\mathbf{l}}, \hat{q}, \hat{g}\}$	14,15,16	29,272

5. Numerical Example

Amongst the five problem types we give a numerical example for the coupled kinetostatics due to its generality. In addition, to validate the completeness of our solution procedure it is customary to pick the parameter set $\psi = \{l_{0i}, \mathbf{a}_i, \mathbf{b}_i, \mathbf{b}_6, \mathbf{F}, \mathbf{M}, k_i\}$ from a known compliant platform solution and check whether this solution is contained in the final obtained solution set. To this end, we first generate a known solution as follows.

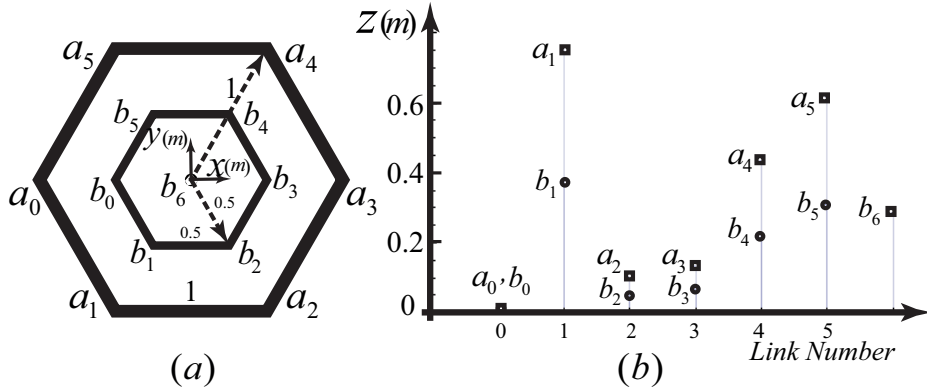


Figure 3: (a) $x - y$ view of the stationary and moving platforms of a compliant Stewart-Gough platform and (b) the z coordinates of the hexagons' vertices

Figure 3(a) depicts the $x - y$ view of the base and the moving platforms of a manipulator where the z components of the vertices of base hexagon are twice those of the moving hexagon which are tabulated in Table 2. Let the quaternion that rotates the stationary plate to the moving plate be $\hat{q} = \frac{1}{\sqrt{30}} (\sqrt{30} \cos(\alpha), \sin(\alpha), 5 \sin(\alpha), 2 \sin(\alpha))$ which is the rotation about the vector $\vec{i} + 5\vec{j} + 2\vec{k}$ with angle $2\alpha = \frac{\pi}{7}$. Moreover, let the quaternion that defines the displacement between a_0 and b_0 be $\hat{g} = (g_0, 4 \sin(\beta), \sin(\beta), 3 \sin(\beta))$ where $g_0 = -\frac{1}{4} \sqrt{15 (5 + \sqrt{5})} \tan(\alpha)$ and $2\beta = 4\frac{\pi}{5}$.

Table 2: The z components of the vertices of the moving platform

b_{0z}	b_{1z}	b_{2z}	b_{3z}	b_{4z}	b_{5z}	b_{6z}
0.00000000	0.37746801	0.05059928	0.06599580	0.21691901	0.30877747	0.28789313

With these prescribed parameters, solution of the kinematic equations (14) gives rise to obtaining the displaced legs length as tabulated in Table 3. Figure 4 illustrates the view of the articulated platform.

Table 3: The displaced legs length of the platform

l_0	l_1	l_2	l_3	l_4	l_5
4.88575729	4.76619210	4.28773288	3.83318455	3.91072136	4.45133028

Moreover, we define $k_i(N/m) = \{20, 35, 25, 45, 30, 40\}$ and $l_{0i}(m) = \{4, 4, 4, 3, 3, 4\}$ as the legs' stiffness and initial length, respectively. These parameters if inserted to Eqs.

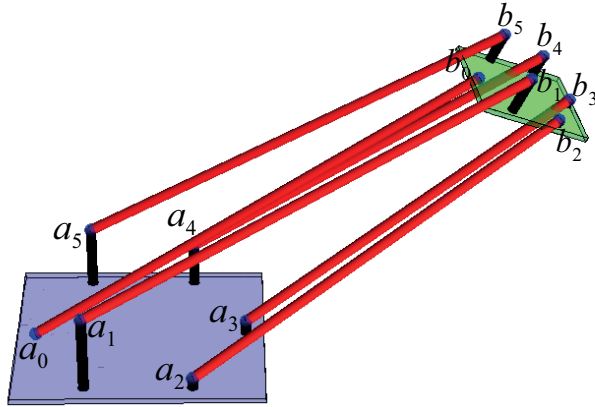


Figure 4: A compliant platform as a known solution

(15) and (16) result in the following force and moment which make the moving platform statically balanced at the given location.

$$\mathbf{F}(N) = \begin{Bmatrix} 116.02858699 \\ 40.77709883 \\ 53.34284663 \end{Bmatrix}, \quad \mathbf{M}(Nm) = \begin{Bmatrix} 9.64921927 \\ -12.97630611 \\ -4.42480924 \end{Bmatrix} \quad (18)$$

Note that the obtained parameters define a statically balanced assembly mode of the articulated compliant platform. Finally, let the parameter set $\psi = \{l_{0i}, \mathbf{a}_i, \mathbf{b}_i, \mathbf{b}_6, \mathbf{F}, \mathbf{M}, k_i\}$ be defined according to these parameters and assume further that $\tilde{\varphi} = \{\hat{q}, \hat{g}, \tilde{l}_i\}$ is still unknown.

Finally, the polynomial system $\mathcal{F}(\tilde{\varphi})$ was solved using Bertini which resulted in 326 real solutions. However, only 10 of them are valid as the obtained solutions should possess positive displaced leg length components. Amongst these, however, one solution is the initial known solution which verifies the completeness of the solution strategy and the remaining 9 solutions listed in Table 4 and further depicted in Figure 5 define new balanced assembly configurations of the same platform.

It is worth mentioning that, for the parameter homotopy devised earlier, the entire polynomial system $\mathcal{F}(\tilde{\varphi})$ was homogenized as the version of Bertini used did not automatically homogenize user-defined homotopies. That is, instead of $\mathbb{C}^6\mathbb{P}^7$, the polynomials were cast in the projective space \mathbb{P}^{13} so as to efficiently distinguish the finite paths from the diverging infinite paths.

6. Conclusions

We studied the finite kinetostatic analysis of a compliant Stewart-Gough platform. The kinetostatic constraint equations were formulated using soma coordinates. To reduce the degree of the resulting constraints, vector dot- and cross-products were cast in quaternion form. We categorized the problems into five problem families. For the most challenging coupled problem, we obtained 13 polynomials with the total degree of 5,971,968. After solving the equations with the numerical polynomial solver Bertini, we reported that the upper bound to the number of finite and nonsingular solutions to the

Table 4: The newly obtained statically balanced assembly configurations

Par.	Sol. 1	Sol. 2	Sol. 3	Sol. 4	Sol. 5	Sol. 6	Sol. 7	Sol. 8	Sol. 9
q_0	-0.00656	-0.00811	-0.17307	-0.06932	-0.00830	0.99985	0.01236	-0.95790	0.89936
q_1	0.34330	0.36748	-0.11739	0.85841	-0.08242	-0.01088	0.93444	-0.02521	0.36491
q_2	-0.86974	-0.01398	0.10554	0.27761	0.98392	0.01308	0.15497	0.26931	-0.24064
q_3	0.35447	-0.92989	0.97218	0.42576	-0.15823	0.00328	-0.32040	0.09620	-0.00901
g_0	-0.04119	0.06327	-0.21112	1.91278	0.27722	0.00355	-0.18485	0.25747	-1.22458
g_1	-0.22465	0.52426	-0.40137	-0.26075	-0.75479	0.30048	0.10310	1.94573	4.34795
g_2	0.38232	0.48224	0.84726	0.43340	0.03696	-0.06311	0.80483	0.98943	2.02488
g_3	1.15488	0.19938	-0.10286	0.55455	0.60843	0.16602	0.68281	0.30369	-0.21979
l_0	1.23777	0.74240	0.96649	2.05477	1.00902	0.34907	1.07647	2.21886	4.95507
l_1	1.67099	0.99774	1.99368	2.38804	0.27797	0.44234	0.83825	2.75142	4.52857
l_2	2.95952	1.84335	3.15096	3.01703	1.74222	0.59166	1.02680	2.95056	4.40092
l_3	4.04082	2.47805	3.81786	3.20988	2.45042	0.70132	0.84205	3.26208	4.02622
l_4	3.89204	2.63018	3.55675	3.14229	1.83657	0.66258	1.81806	3.19465	3.97829
l_5	2.73199	1.93971	2.40323	2.85478	0.76758	0.51481	1.91988	2.80623	4.30487

coupled kinetostatics is 29,272. A numerical example was studied for which the parameters were picked from a known compliant mechanism solution. Other than the known solution, nine new statically balanced assembly configurations of the initial compliant mechanism were obtained.

Acknowledgments

The authors are grateful to the anonymous reviewers for the mindful comments. The authors acknowledge the University of Maryland, Baltimore County, for the computer-time on their high performance computing facility (HPCF-tara). The first author would like to thank a few individuals; Dr. C.W. Wampler for the helpful comments, Mr. A. Knister for the assistance on compiling Bertini on tara and Prof. Matthias K. Gobbert, the chair of the UMBC HPCF, for his generosity on providing the extra computer-time usage. This work is supported by National Science Foundation under Grant (CMMI-0845793).

References

- [1] V. E. Gough, Contribution to discussion of papers on research in Automobile Stability, Control and Tyre performance, Proc. Auto Div. Inst. Mech. Eng. (1956) 392–394.
- [2] D. Stewart, A Platform with Six Degrees of Freedom, Proc. Institution of Mechanical Engineers (UK) 180, Part 1, No. 15 (1965) 371–376.
- [3] J. P. Merlet, Parallel Robots, Springer, Netherlands, 2006.
- [4] C. D. C. III, J. Duffy, J. C. Correa, Static Analysis of Tensegrity Structures, Journal of Mechanical Design 127 (2) (2005) 257–268.
- [5] J. Bayat, C. D. C. III, Closed-Form Equilibrium Analysis of Planar Tensegrity Structures, ASME Conference Proceedings 2007 (48094) (2007) 13–23.

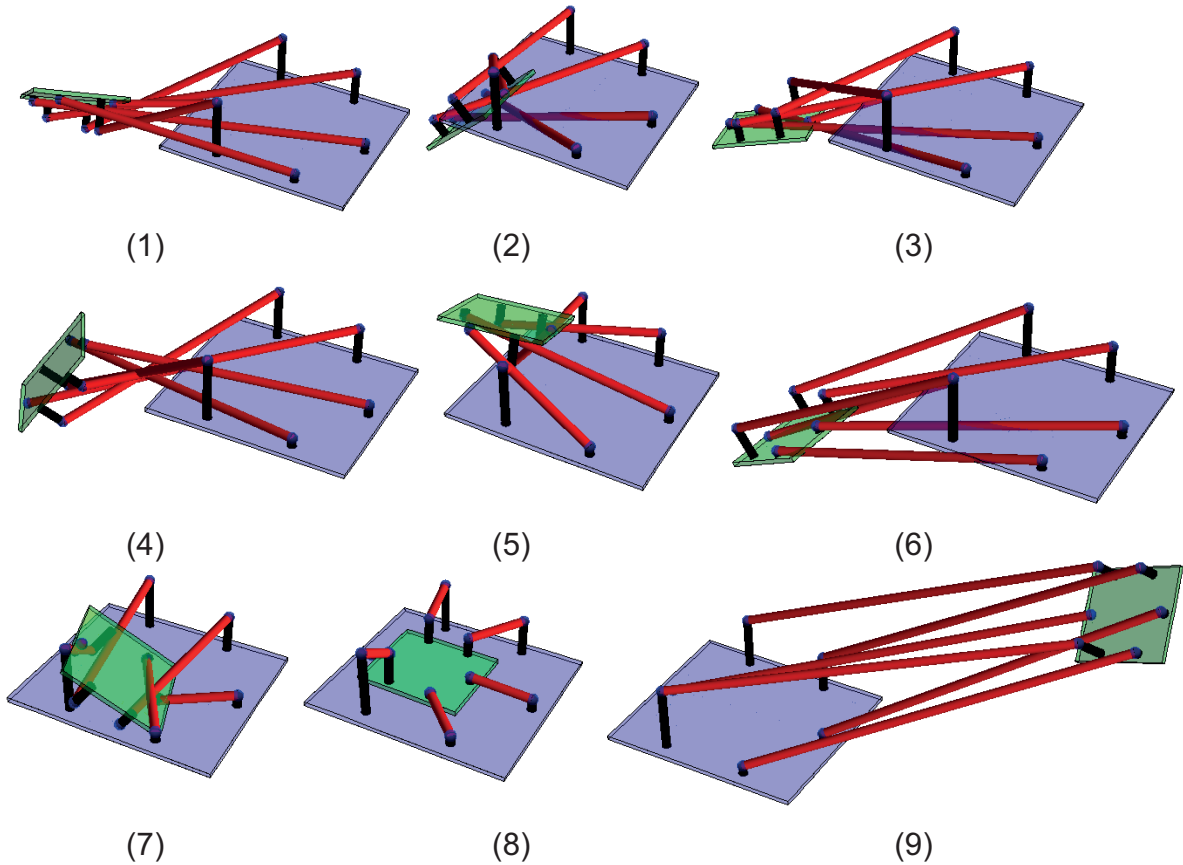


Figure 5: The obtained nine new solutions

- [6] M. Arsenault, C. M. Gosselin, Static Balancing of Tensegrity Mechanisms, ASME Journal of Mechanical Design 129 (3) (2007) 295–300.
- [7] D. E. Whitney, Remote Center Compliance, in: J. Diponio, Y. Hasegawa (Eds.), Encyclopedia of Robotics System and Control, vol. 2, Industrial Training Co., 1316–1324, 1986.
- [8] M. Carricato, C. M. Gosselin, A Statically Balanced Gough/Stewart-Type Platform: Conception, Design, and Simulation, ASME Journal of Mechanisms and Robotics 1 (3) (2007) 031005.
- [9] M. Raghavan, The Stewart Platform of General Geometry Has 40 Configurations, Journal of Mechanical Design 115 (2) (1993) 277–282.
- [10] A. P. Morgan, Solving Polynomial Systems Using Continuation for Scientific and Engineering Problems, Prentice-Hall, Englewood Cliffs, NJ, 1987.
- [11] E. L. Allgower, K. Georg, Introduction to Continuation Methods, SIAM, Philadelphia, 2003.

- [12] T. Y. Li, Numerical Solution of Polynomial Systems by Homotopy Continuation Methods, *Handbook of Numerical Analysis* 11 (1) (2003) 209–304.
- [13] A. J. Sommese, C. W. Wampler, *The Numerical Solution of Systems of Polynomials arising in Engineering and Science*, World Scientific Press, Singapore, 2005.
- [14] J. C. Faugère, D. Lazard, Combinatorial classes of parallel manipulators, *Mechanism and Machine Theory* 30 (6) (1995) 765 – 776.
- [15] B. Mourrain, The 40 “generic” positions of a parallel robot, in: *Proceedings of the 1993 international symposium on Symbolic and algebraic computation*, ISSAC93, ACM, New York, NY, USA, 173–182, 1993.
- [16] C. W. Wampler, Forward displacement analysis of general six-in-parallel sps (Stewart) platform manipulators using soma coordinates, *Mechanism and Machine Theory* 31 (3) (1996) 331 – 337.
- [17] O. Bottema, B. Roth, *Theoretical Kinematics*, Dover Publications, INC, 1979.
- [18] M. L. Husty, An algorithm for solving the direct kinematics of general Stewart-Gough platforms, *Mechanism and Machine Theory* 31 (4) (1996) 365 –379.
- [19] C. Innocenti, Forward Kinematics in Polynomial Form of the General Stewart Platform, ASME, *Journal of Mechanical Design* 123 (2) (2001) 254–260.
- [20] T.-Y. Lee, J.-K. Shim, Improved dialytic elimination algorithm for the forward kinematics of the general Stewart-Gough platform, *Mechanism and Machine Theory* 38 (6) (2003) 563 – 577.
- [21] D. Gan, Q. Liao, J. S. Dai, S. Wei, L. D. Seneviratne, Forward displacement analysis of the general 6-6 Stewart mechanism using Gröbner bases, *Mechanism and Machine Theory* 44 (9) (2009) 1640 – 1647.
- [22] H. Tari, H.-J. Su, A Secant Homotopy Solution Library for the Forward Kinematics of Stewart-Gough Platforms, *Journal of Mechanical Design*, Submitted .
- [23] D. J. Bates, J. D. Hauenstein, A. J. Sommese, C. W. Wampler, Bertini: Software for Numerical Algebraic Geometry, <http://www.nd.edu/~sommese/bertini>, 2011.
- [24] T. Patterson, H. Lipkin, Structure of robot compliance, *ASME Journal of Mechanical Design* 115 (3) (1993) 576–580.
- [25] S. Huang, J. M. Schimmels, The duality in spatial stiffness and compliance as realized in parallel and serial elastic mechanisms, *ASME Journal of Mechanical Design* 124 (1) (2002) 76–84.
- [26] T. M. Pigoski, J. Duffy, An Inverse Force Analysis of a Planar Two-Spring System, *Journal of Mechanical Design* 117 (4) (1995) 548–553.

- [27] L. Sun, C. G. Liang, Q. Z. Liao, A reverse static force analysis of a special planar three-spring system, *Mechanism and Machine Theory* 32 (5) (1997) 609 – 615.
- [28] H.-J. Su, J. M. McCarthy, A Polynomial Homotopy Formulation of the Inverse Static Analysis of Planar Compliant Mechanisms, *ASME Journal of Mechanical Design* 128 (4) (2006) 776–786.
- [29] Y. Zhang, C. Liang, J. Duffy, E. J. F. Primrose, A reverse force analysis of a spatial three-spring system, *Mechanism and Machine Theory* 32 (6) (1997) 667 – 678.
- [30] D. J. Bates, J. D. Hauenstein, A. J. Sommese, C. W. Wampler, Software for numerical algebraic geometry: a paradigm and progress towards its implementation, *Software for Algebraic Geometry*, The IMA Volumes in Mathematics and its Applications 148 (2008) 1–14.
- [31] J. D. Hauenstein, A. J. Sommese, C. W. Wampler, Regeneration Homotopies for Solving Systems of Polynomials, *Mathematics of Computation* 80 (2011) 345–377.
- [32] A. Griewank, A. Walther, *Evaluating Derivatives: Principles and Techniques of Algorithmic Differentiation*, SIAM, Philadelphia, PA, 2nd edn., 2008.